BULLETIN OF THE POLISH ACADEMY OF SCIENCES
TECHNICAL SCIENCES, Vol. 74(5), 2026, Article number: 1148
DOI: 10.24425/bpasts.2026.1148

Conceptual design and functional verification of a novel torque vectoring drive-axle for electric vehicles

Shoulin GAO[1], Qingfa GE[1], Liwei SHI[1], Dong XIAO[1], Jianlong HU[2]*, and Zewen YANG[1]

[1] School of Transportation and Vehicle Engineering, Shandong University of Technology, Zibo 255000, China
[2] Qingdao Qingte Zhongli Axle Co., Ltd, Qingdao 266041, China

Abstract. The conventional power transmission system of electric vehicles typically distributes driving torque equally between the left and right wheels, which restricts the potential to enhance the vehicle's chassis dynamic performance. To solve this problem, a novel torque vectoring drive-axle (TVDa) is proposed, and it can achieve the driving torque precise distribution between the two-side wheels, thereby effectively improving the vehicle's active safety and handling stability. Firstly, the structure design principle and torque distribution mechanism of the novel TVDa is theoretically analyzed in this paper, and establishes the design criteria for key structural parameters. Secondly, the motor parameters of the TVDa are systematically matched to meet the practical application requirements of the vehicle. Next, a virtual prototype model of an electric vehicle equipped with the TVDa is built, and the functional feasibility of the TVDa impact on vehicle dynamic performance is verified. Finally, simulation results demonstrate that the novel TVDa can significantly improves the vehicle's maneuverability and trafficability through distributing driving torque between the two-side wheels, while maintaining low energy consumption in the torque vectoring motor, indicating strong potential for engineering applications.

Keywords: electric vehicle, torque vectoring, electric drive-axle, virtual prototype, vehicle dynamic performance.

1. INTRODUCTION

At present, the active safety and handling stability of vehicles are a source of increasing concern for people, and utilizing additional yaw moment is the main way to achieve vehicle electronic stability control. Examples include Bosch's electronic stability control (ESC) system and Nissan's vehicle dynamics control (VDC) System. However, ESC and VDC can effectively enhance the vehicle's driving safety and handling stability mainly through independent control of braking force for each wheel [1, 2]. Due to the decrease in vehicle power and increase in frictional energy consumption during the braking process [3], such system is only suitable for deceleration or an extreme cornering situation, which affects the maneuverability and driving pleasure of vehicles under constant speed and acceleration cornering conditions [4].

In recent years, wheel torque vectoring (TV), as an advanced emerging technology, received increasing attention in the automotive industry. The TV technology can achieve arbitrary transfer and distribution of driving torque on each wheel according to the actual needs of the vehicle, thus effectively improving the active safety and "fun-to-drive" qualities of the vehicle [5, 6]. Compared with the traditional way of achieving stability control through braking force, the TV drive technology transmits torque instead of reducing torque between the inter-wheels, so it can achieve higher system control efficiency and better vehicle driving pleasure. The distributed drive electric vehicle (DDEV), equipped with a motor on each wheel, has advantages of independent and precise control of wheel torque. Therefore, the DDEV is inherently suitable for TV drive technology implementation, and also considered to be the best driving form of the future automobile chassis [7, 8]. However, due to the limitation of key technical problems such as the in-wheel motor heat dissipation, high manufacturing cost and the increase of unsprung mass, which are all difficult to solve, the DDEV has not been widely applied at present [9]. Therefore, how to implement TV drive technology on the basis of a traditional electric vehicle drive system, is a problem worth studying.

Nowadays, the electric vehicles drive system commonly employs the form of motors centralized arrangement, and distributes the power source motor output torque to the left and right wheels through an open differential device [10]. However, the open differential always distributes the driving torque equally to the two-side wheels, and when the vehicle is driving on uneven roads or off-road surfaces, it is prone to cause the low adhesion side wheels slipping while the high adhesion side wheels lose power [11, 12]. This type of working characteristic is not conducive to improving the passing ability of the vehicle on bad roads and the handling stability under turning conditions. Therefore, the drive system based on the open differential cannot meet the technical requirements for developing high-performance electric vehicles in the future.

*e-mail: hujianlong163@163.com

Manuscript submitted 2025-12-23, revised 2026-05-08, initially accepted for publication 2026-05-19, published in September 2026.

To overcome the technical constraints of conventional open differential while achieving controlled torque distribution across wheels, many automobile enterprises have developed differentials with driving torque transfer function, such as TORSEN differential [13] and passive limited slip differential [14, 15], etc. When the speed difference between the inter-wheels exceeds a definite threshold, this type of differential can transform the driving torque from the high-speed side to the low-speed side through the locking force generated internally, thereby preventing excessive slippage of the wheels on low adhesion side, and thus promote the vehicle's power performance. However, such passive differentials permit only unidirectional torque transmission-specifically from the wheel with higher rotational speed to that with lesser speed. According to the Ackerman steering principle, at the moment of vehicle turning, the rotational speed of the outer wheels is usually higher than that of the inner wheels. Therefore, the driving torque of the vehicle is always transferred from the outer wheels to the inner wheels, which would generate an additional moment that is not conducive to the yaw motion and affects the steering maneuverability of the vehicle.

To achieve bidirectional controllable distribution of driving torque in a centralized electric drive system, torque vectoring differential (TVD) has been increasingly adopted in high chassis dynamic performance vehicles in recent years. The representative technology schemes include super all wheel control (S-AWC) of Mitsubishi [16], super handling-all wheel drive (SH-AWD) of Honda [17], sports differential of Audi [18] and torque vectoring drive-axle of BWM [19]. Many experts also studied the innovative structural configuration and vehicle application technology of TVD. Yu *et al*. [20] designed a novel torque vectoring electric drive system utilizing the Ravigneaux gearset mechanism, and the working principle and function are simulated and verified based on SimulationX software. Lin *et al*. [21] proposed a hybrid torque-vectoring differential (H-TD), the H-TD adds a motor and clutch device on the basis of the traditional internal combustion engine drive system. By controlling the clutch working state, the torque coupling or torque vectoring function of the motor, output power between the two-side wheels can be achieved. Diachuk *et al*. [22] presented an alternative mathematical method, the differential dynamic equation of the Audi sport differential mechanism was established, and its dynamic characteristics was numerically calculated and analyzed. Amin *et al*. [23] developed a vehicle integrated control system using TVD and ESC to improve the vehicle's active safety and steering ability, and the research indicates that the designed control strategy can significantly enhance the vehicle's turning maneuverability at low speeds and driving stability at high speeds.

In summary, the TVD literature mentioned above generally adopts friction components such as brakes or clutches to realize the distribution of wheel driving torque, and the typical TVDs structure schemes are shown in Fig. 1. This type of TVDs have technical weaknesses in the following two aspects: 1) during the operation process, the clutch is subject to slipping and heating, resulting in more energy loss, which would affect the transmission efficiency of the TVDs system; 2) due to the torque one-way transmission characteristics of the clutch, that is that the torque can only be transmitted from the high-speed side to the low-speed side, this type of TVDs usually install two identical actuators on both sides of the differential to achieve torque distribution function, thus significantly increasing the cost and weight of the drive-axle.

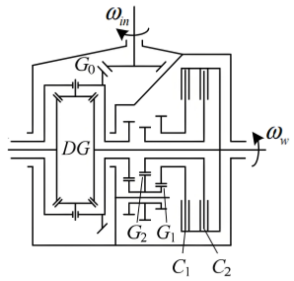

ω_{in} - input shaft speed; ω_w - output shaft speed; C_1-left side clutch; C_2-right side clutch; G_0-reducer; G_1-left gear pairs; G_2-right gear pairs; *DG*-differential

(a) Mitsubishi S-AWC [16]

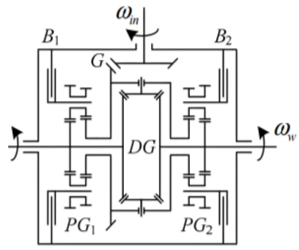

ω_{in} - input shaft speed; ω_w - output shaft speed; B_1-left side braker; C_2-right side braker; G_0-reducer; G_1-left gear pairs; G_2-right gear pairs; *DG*-differential

(b) Honda SH-AWD [17]

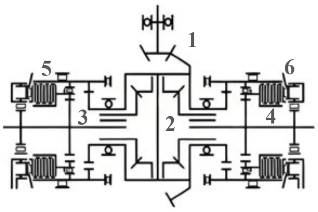

1- reducer; 2- differential; 3-left gear pairs; 4-left gear pairs; 5-left side clutch; 6-right side clutch

(c) Audi sports differential [18]

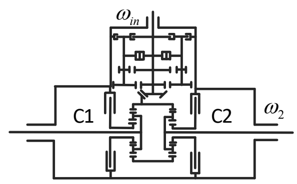

ω_{in}- input shaft speed; ω_1- left half shaft speed; ω_{12}- right half shaft speed; C1-left side clutch; C2-left side clutch

(d) BMW drive-axle [19]

Fig. 1. Typical TVDs schematic structure

To solve the above problems existing in TVDs, a novel type of TVDa is proposed in this paper, and its principle and function are analyzed and verified. Specifically, the major innovations or contributions of the paper are as below.

1. A novel TVDa structure scheme is proposed, which can distribute driving torque between the two-side wheels according to the vehicle's dynamic control requirements. Furthermore, the design methodology for its structural and motor parameters is established.
2. A virtual vehicle simulation platform incorporating the TVDa was developed. Using this platform, the operating mechanism and functional feasibility of the novel TVDa's impact on vehicle dynamics were verified.

The rest of paper is organized as follows. In Section 2, the structure design principle and working mechanism of TVDa is analyzed. The motor system parameters are matched in Section 3. In Section 4, the vehicle virtual simulation platform is built. The working mechanism and function of TVDa are verified in Section 5. Finally, research conclusions are presented in Section 6.

2. STRUCTURE DESIGN PRINCIPLE AND WORKING MECHANISM ANALYSIS OF TVDA

On the basis of the traditional electric drive system structure, a novel TVDa that can achieve controllable torque distribution between wheels is proposed, and the structural design principle and working mechanism of TVDa are analyzed in detail.

2.1. Structural design principle analysis of TVDa

Traditional electric vehicles adopt a centralized layout drive system, with its structural representation depicted in Fig. 2a, which primarily consists of the main drive motor, main reducer, open differential, left-half shaft and right-half shaft. The main drive motor output torque first goes through the speed deceleration and torque increasing effect of the main reducer, and finally it is evenly distributed to two-side half shafts by the open differential configuration. To overcome the disadvantage of open differential driving torque always being evenly distributed, while retaining the fundamental structure of traditional electric drive system, a novel TVDa structure scheme is proposed, which mainly increases the TV motor, planetary gear set and TV gear unit, so as to achieve the torque vectoring function between two-side wheels. The structure schematic diagram of TVDa is presented in Fig. 2b.

As depicted in Fig. 2, the novel TVDa utilizes an inner-rotor hollow-shaft permanent magnet synchronous motor (PMSM)

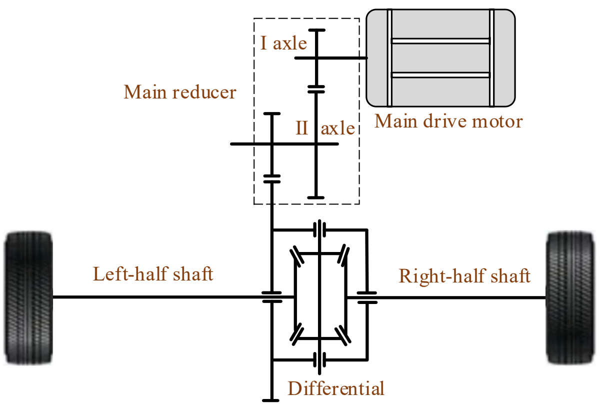

(a) traditional electric drive system

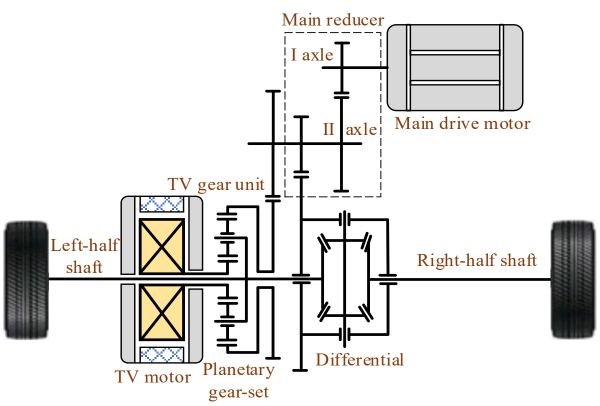

(b) novel TVDa

Fig. 2. Structure schematic diagram of electric drive system

as the TV motor, and its output shaft is directly connected with the sun gear of planetary gear set. The planet carrier links to the left-half shaft of TVDa. The TV gear unit's driving gear is mounted concentrically outside the planetary ring gear, with its driven gear fixed to the main reducer's second axle.

2.2. Working mechanism analysis of TVDa

(1) Speed transmission relationship analysis

The speed of all the rotational elements of planetary gear set, TV gear unit and differential gear unit can be visualized in the velocity diagram as presented in Fig. 3. According to the proportional relationship of each node in Fig. 3, the speed of TVDa components during the vehicle driving process can be intuitively obtained.

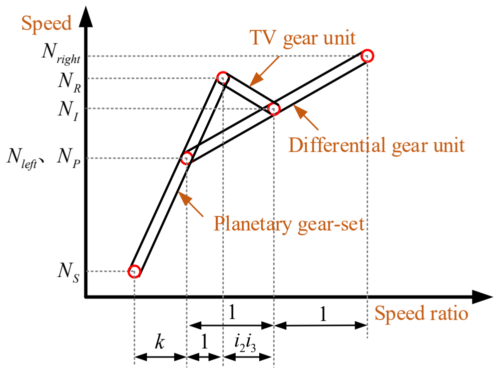

Fig. 3. TVDa velocity diagram

Assuming that the speed difference between the inter-wheels during the turning process of the vehicle is ΔN, then the two-side half shafts speed can be calculated as:

$$\begin{aligned} N_{\text{right}} &= N_I + \frac{\Delta N}{2}, \\ N_{\text{left}} &= N_I - \frac{\Delta N}{2}, \\ N_I &= \frac{N_m}{i_1 i_2}, \end{aligned} \tag{1}$$

where, N_I is the differential housing speed; N_m is the main drive motor speed; and i_1 and i_2 are the two-stage reduction ratios of the main reducer.

The ring gear speed can be obtained by using the lever balance principle in the velocity diagram, which can be expressed as:

$$N_R = i_3 i_2 N_I = \frac{i_3 N_m}{i_1}, \tag{2}$$

where, i_3 is the transmission ratio of TV gear unit.

Consequently, based on the kinematic relationship among system components, the TV motor rotational speed is derived as:

$$\begin{aligned} & N_S + kN_R - (1+k)N_P = 0, \\ & N_P = N_{\text{left}}, \\ & N_S = N_{tv} = \frac{(1+k-i_2 i_3 k)N_m}{i_1 i_2} - \frac{(1+k)}{2}\Delta N, \end{aligned} \tag{3}$$

where, N_S represents the speed of the sun gear in the planetary gear set; N_P is the speed of the planet carrier in the planetary gear set; k is the characteristic parameter of the planetary gear set, and it represents the ratio of the number of ring gear teeth to the number of sun gear teeth.

(2) Driving torque distribution principle analysis

When two power source motors output torque simultaneously, the torque flow direction of the TVDa is shown in Fig. 4. According to the torque transfer relationship of each component, the driving torque transfer amount between the inter-wheels can be obtained.

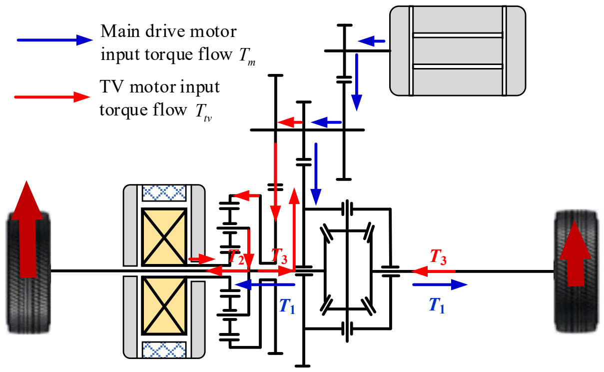

Fig. 4. Torque flow of TVDa

Under the TV motor non-operational conditions, the torque transmitted from the main drive motor output torque T_m to the two-side half shaft is expressed as follows:

$$T_1 = \frac{i_1 i_2 T_m}{2}. \tag{4}$$

The torque transmitted from the TV motor output torque T_{tv} to the left-half shaft through the planetary carrier of planetary gear set is defined as T_2, which can be calculated as:

$$T_2 = (1+k)T_{tv}. \tag{5}$$

The TV motor output torque T_{tv} passes through the ring gear of planetary gear set, TV gear unit and differential gear unit in sequence and is finally transmitted to the two-side half shafts, which is defined as T_3, and can be expressed as:

$$T_3 = \frac{k i_3 i_2 T_{tv}}{2}. \tag{6}$$

Therefore, during the two power source motors synchronous operation, the distributed output torques on the half shaft are derived as:

$$\begin{aligned} T_{\text{right}} &= T_1 + T_3 = \frac{i_1 i_2 T_m}{2} - \frac{k i_2 i_3 T_{tv}}{2}, \\ T_{\text{left}} &= T_1 + T_2 + T_3 = \frac{i_1 i_2 T_m}{2} + (1+k)T_{tv} - \frac{k i_2 i_3 T_{tv}}{2}. \end{aligned} \tag{7}$$

From the above formula, it can be seen that if the TV motor operation does not affect the main drive motor output torque, the following conditions should be satisfied:

$$\begin{aligned} T_{\text{right}} + T_{\text{left}} &= i_1 i_2 T_m, \\ (1+k)T_{tv} - \frac{k i_2 i_3 T_{tv}}{2} &= \frac{k i_2 i_3 T_{tv}}{2}. \end{aligned} \tag{8}$$

From the above formula, if $i_3 = (1+k)/(k i_2)$, the two-side half shafts output torque can be re-expressed as:

$$\begin{aligned} T_{\text{right}} &= \frac{i_1 i_2 T_m}{2} - \frac{(1+k)T_{tv}}{2}, \\ T_{\text{left}} &= \frac{i_1 i_2 T_m}{2} + \frac{(1+k)T_{tv}}{2}. \end{aligned} \tag{9}$$

At this time, according to (3), the TV motor speed can be obtained:

$$N_S = \frac{(1+k)\Delta N}{2}. \tag{10}$$

To summarize, the total driving torque and differential torque of TVDa are defined by:

$$\begin{aligned} T &= T_{\text{left}} + T_{\text{right}} = i_1 i_2 T_m, \\ \Delta T &= T_{\text{left}} - T_{\text{right}} = (1+k)T_{tv}. \end{aligned} \tag{11}$$

Based on the above theoretical analysis, the proposed novel TVDa demonstrates two distinct advantages.

i) TVDa employs a fully mechanical transmission design, eliminating the clutches and brakes required in the conventional TVD system. This innovative architecture offers superior transmission efficiency, enhanced reliability, improved integration and significant engineering application value.

ii) Through reasonable design of the TV gear unit's transmission ratio, the novel TVDa enables arbitrary torque transfer with both in magnitude and direction, between the bilateral wheels while maintaining constant total driving torque. Crucially, the system decouples control of the total driving torque (managed by the main motor) and differential torque (regulated by the TV motor), achieving independent and precise coordination of the vehicle's longitudinal and lateral dynamics. It also significantly enhances controllability as compared to conventional TVDs.

2.3. Working mechanism of TVDa simulation verification

(1) Speed transmission relationship verification

To verify the correctness of the speed relationship of TVDa components based on theoretical analysis, the TVDa virtual prototype model is built in SimulationX software. SimulationX is a physics system simulation software that support multiple disciplines, and it provides comprehensive solutions from conceptual design to verification, which can improve system development efficiency and reduce development costs [24, 25]. In Fig. 5, the two-half shafts input pre-determined target speed, and the speed change of the TV motor and main drive motor is measured through the speed sensor. The structural parameters of TVDa are illustrated in Table 1.

Figure 6 shows the TVDa speed principle simulation results. During synchronous rotation of the two-side half shafts, the TV motor speed is zero. When the two-side half shafts speed

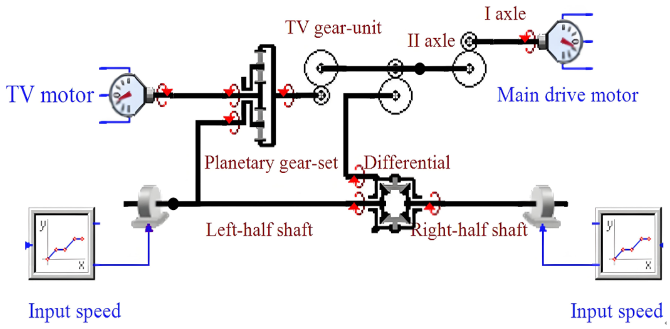

Fig. 5. Virtual simulation model of TVDa speed principle verification

difference is 50 rpm, that is, $\Delta N = 50$ rpm, the TV motor speed is -125 rpm, indicating that the simulation results are consistent with (10).

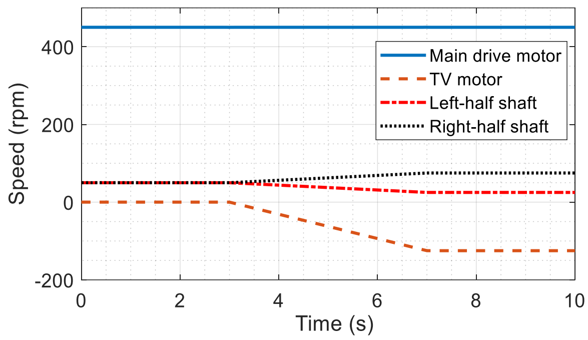

Fig. 6. Speed principle simulation results

(2) Driving torque distribution principle verification

To validate the torque distribution principle between wheels of TVDa, a virtual prototype simulation model is developed, as shown in Fig. 7. The motors are used as power source input torque of TVDa, and the output torque is measured by the torque sensor.

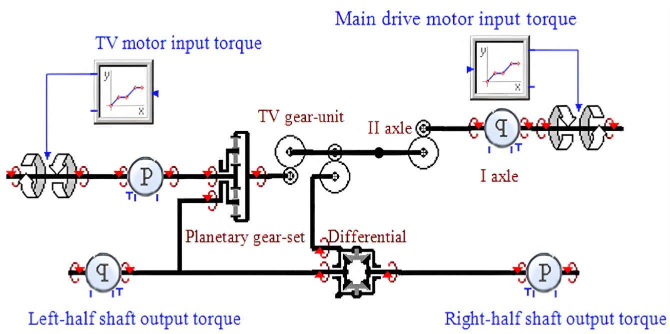

Fig. 7. Virtual prototype model of TVDa torque distribution principle verification

The simulation results of torque distribution principle of TVDa are illustrated in Fig. 8. When only the main drive motor is working, the left- and right-half shaft output torque remain consistent. At the third second, the TV motor starts to work and outputs torque, the wheel driving torque is transferred and distributed at this time, but the total driving torque remains unchanged. The simulation results are consistent with (11), which indicates the correctness of the above theoretical analysis.

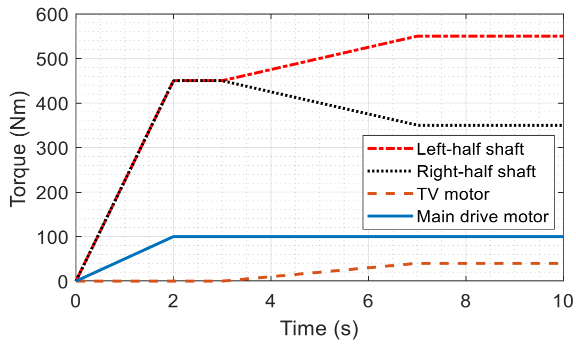

Fig. 8. Torque distribution principle simulation results

3. MOTOR PARAMETER MATCHING OF TVDA

To better satisfy the requirements of vehicle application, this section presents a matching design for the motor system parameters of the proposed novel TVDa.

3.1. Parameter matching of main drive motor

This paper takes B-class electric vehicle with rear axle drive system as the target model for the application of novel TVDa, and the basic parameters and performance indicators can be found in Table 1.

Table 1
Specifications of the vehicle [26]

Parameter	Value
Mass m (kg)	1560
Wheelbase L (m)	2.68
Wheel track b (m)	1.68
Wheel rolling radius R_w (m)	0.30
Yaw moment of inertia I (kg m^2)	1530
Center of mass height h (m)	0.55
First reduction ratio of main reducer i_1	3
Second reduction ratio of main reducer i_2	3
Transmission ratio of TV gear unit i_3	0.42
Planetary gear set characteristic parameters k	4
Frontal area A (m^2)	2.1
0 to 100km/h acceleration time t_{100} (s)	6–8
Maximum climbing gradient α_{max} (%)	≥ 30
Maximum speed V_{max} (km h^{-1})	≥ 150

The main drive motor maximum output power of TVDa must meet the need of vehicle power performance requirements. The vehicle power requirements under the condition of meeting the maximum speed is calculated as [26]:

$$P_{V\max} \geq \frac{mgf}{3600}V_{\max} + \frac{C_D A}{76140}V_{\max}^3, \tag{12}$$

where, f represents the rolling resistance coefficient and C_D denotes the air resistance coefficient.

To satisfy the vehicle's maximum gradeability requirement, the power demand of the main drive motor is formulated as [26]:

$$P_{\alpha\max} \geq \frac{mgf\cos\alpha_{\max}}{3600}V_i + \frac{mg\sin\alpha_{\max}}{3600}V_i + \frac{C_D A}{76140}V_i^3, \tag{13}$$

where, V_i represents stable vehicle speed, usually set to 30 km/h.

To satisfy the vehicle's maximum acceleration requirement, the power demand is given by [26]:

$$P_{i\max} \geq \frac{1}{3600t_m}\left(\frac{\delta m V_m^2}{2\cdot 3.6} + mgf\int_0^{t_m} V_m\left(\frac{t^{0.5}}{t^{0.5}}\right)\mathrm{d}t + \frac{C_D A}{21.5}\int_0^{t_m} V_m^3\left(\frac{t^{1.5}}{t^{1.5}}\right)\mathrm{d}t\right), \tag{14}$$

where, t_m represents the vehicle 0–100 km/h acceleration time and V_m represents the vehicle target speed.

The maximum output torque of main drive motor should meet the requirement of the vehicle maximum gradeability [26].

$$T_{m\_\max} \geq \frac{R}{i_0}\left(mg\sin\alpha_{\max} + mgf\cos\alpha_{\max} + \frac{C_D A}{21.15}V_i^2\right), \tag{15}$$

where, i_0 represents the transmission ratio of the main reducer.

The main drive motor peek speed must meet the requirements of the vehicle maximum vehicle speed [26].

$$N_{m\_\max} \geq \frac{V_{\max} i_0}{0.377R_w}. \tag{16}$$

3.2. Parameter matching of TV motor

To maximize vehicle dynamic performance enhancement, the proposed novel TVDa system must be able to completely transfer the torque from one side wheels to the other side wheels. Consequently, the TV motor's peak torque output requirement is given by:

$$T_{tv\_\max} = \frac{i_1 i_2}{1+k}T_{m\_\max}. \tag{17}$$

During the steering process, we assume that that electric vehicle equipped with TVDa is a rigid body, that is, ignoring the tilting or pitching motion caused by suspension and other components. To guarantee stable cornering performance of the vehicle, the rotational speed of four wheels should meet the Ackermann steering geometry relationship [27], the vehicle ideal steering kinematic model, as shown in Fig. 9.

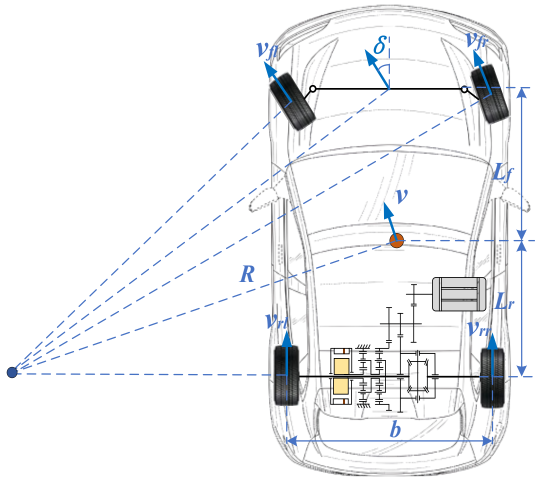

Fig. 9. Ackermann turning geometric model

As shown in Fig. 9, during the turning process of the vehicle, the wheels rotational speed is derived as:

$$\begin{aligned}
vfl &= \frac{v\sqrt{L^2+\left(\frac{L}{\tan\delta}-\frac{b}{2}\right)^2}}{\sqrt{L_r^2+(L/\tan\delta)^2}},\\
vfr &= \frac{v\sqrt{L^2+\left(\frac{L}{\tan\delta}+\frac{b}{2}\right)^2}}{\sqrt{L_r^2+(L/\tan\delta)^2}},\\
vrl &= \frac{v\sqrt{\frac{L}{\tan\delta}}-b}{2\sqrt{L_r^2+(L/\tan\delta)^2}},\\
vrr &= \frac{v\sqrt{\frac{L}{\tan\delta}}+b}{2\sqrt{L_r^2+(L/\tan\delta)^2}},\\
L &= L_r + L_f,
\end{aligned} \tag{18}$$

where, v is the vehicle centroid velocity; δ is the average steering angle of front wheels; vfl, vfr, vrl, vrr is the wheel rotational speed of left front, right front, left rear and right rear, respectively; R is the turning radius; L_r, L_f are the center of mass location from the front and rear axles, respectively.

Therefore, the maximum speed difference of the left and right rear wheels can be obtained from:

$$\Delta N_{\max} = v_{rr} - v_{rl} = \frac{V_{\max} b}{3.6R_{\min}}\cdot\frac{60}{2\pi R_w}, \tag{19}$$

where, $R_{\min}$ represents the vehicle's minimum turning radius.

By combining (10) and (19), the peak operational speed requirement of the TV motor is formulated as:

$$N_{tv\_\max} = \left|-(1+k)\Delta N_{\max}/2\right|. \tag{20}$$

Based on the above calculated theory, the motor parameters of the novel TVDa are shown in Table 2.

Table 2
Motor parameters

Parameter	Main drive motor	TV motor
Peak power (kW)	130	30
Rated power (kW)	75	20
Peak torque (Nm)	370	540
Peak speed (rpm)	13000	1000
Rated speed (rpm)	5000	400

According to the motor parameters matched in Table 2, the motors' external characteristic and efficiency characteristic curves are shown in Fig. 10.

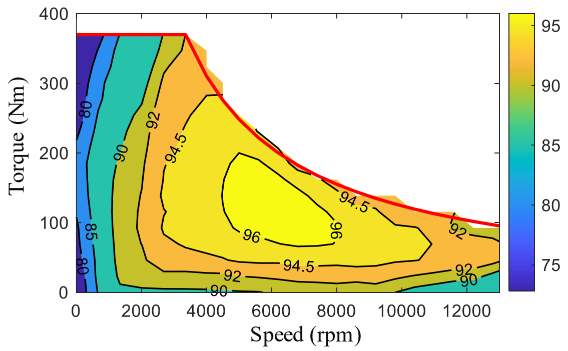

(a) main drive motor

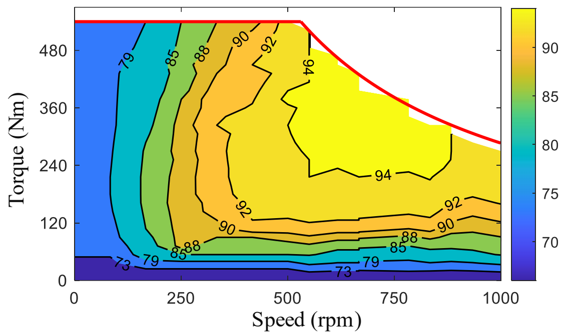

(b) TV drive motor

Fig. 10. Motor characteristic curve

4. DYNAMIC MODELING OF VEHICLE

In this section, the dynamic equations of the electric vehicle are derived to provide a simulation platform for functional verification of the TVDa.

4.1. Vehicle body dynamics model

To analyze the functional feasibility of novel TVDa wheel torque distribution function on the vehicles dynamic performance quality, a vehicle dynamics model that ignores body pitch and vertical motion is established. The longitudinal, lateral and yaw motions dynamic formulas are derived as [28]:

$$m(\dot{u}-v\gamma) = F_{x2}+F_{x4}-(F_{y1}+F_{y3})\sin\delta_f - \frac{1}{2}\rho C_D A u^2, \tag{21}$$

$$m(\dot{v}+u\gamma) = F_{y2}+F_{y4}+(F_{y1}+F_{y3})\cos\delta_f, \tag{22}$$

$$I_z\dot{\gamma} = (F_{y1}+F_{y3})L_f\cos\delta_f - (F_{y2}+F_{y3})L_r + \frac{b}{2}(F_{y1}-F_{y3})\sin\delta_f + \frac{b}{2}(F_{x2}-F_{x4}), \tag{23}$$

where, u is the longitudinal velocity; v is the lateral velocity; γ represent the yaw rate; F_{xi} and F_{yi} are the longitudinal and lateral tire forces of the th wheel, respectively; I_z is the yaw moment of inertia; and δ_f is the front wheel steering angle.

The rotational motion dynamics formula of driving wheels is derived as [28]:

$$I_{wi}\dot{\omega}_i = T_i - F_{xi}R_w, \quad i = rl,\ rr, \tag{24}$$

where, I_{wi} denotes the th wheel rotational inertia; ω_i and T_i stand for the rotational speed and wheel torque; and R_w is the wheel rolling radius.

The slipping state of driving wheels is indicated as follows [28]:

$$s_i = \frac{R_w\omega_i - V_i}{V_i}, \tag{25}$$

where, V_i represents the wheel center linear speed.

4.2. Tire model

The tire model is used to describe the force transmission relationship between the tire and road surface. Specifically, the Magic Formula tire model provides accurate representations of longitudinal force and lateral force through a unified trigonometric formulation. This has the advantage of concise expression and fewer unknown parameters involved. The pure longitudinal lateral tire forces without considering the longitudinal and lateral slip, respectively, are modeled as follows [29]:

$$\begin{aligned} F_{x0} &= \lambda F_{zi}\Big(C_x \arctan\big(B_x s - E_x\left(B_x s - \arctan(B_x s)\right)\big)\Big), \\ F_{y0} &= \lambda F_{zi}\Big(C_y \arctan\big(B_y\alpha - E_y\left(B_y\alpha - \arctan(B_y\alpha)\right)\big)\Big), \end{aligned} \tag{26}$$

where, C_x, B_x, E_x, C_y, B_y and E_y represent the tire characteristic parameters; λ represents the road adhesion coefficient; F_{zi} $(i = (1{-}4)$ is the wheel vertical load.

Considering vertical load transfer of each wheel caused by longitudinal and lateral acceleration during vehicle turning, based on the moment balance relationship, the wheels vertical load is expressed as [28]:

$$
\begin{aligned}
F_{z1} &= mgL_r/2\left(L_f+L_r\right)-m\dot{u}h/2\left(L_f+L_r\right)\\
&\quad -\ m\dot{v}hL_r/b\left(L_f+L_r\right),\\
F_{z2} &= mgL_f/2\left(L_f+L_r\right)-m\dot{u}h/2\left(L_f+L_r\right)\\
&\quad +\ m\dot{v}hL_r/b\left(L_f+L_r\right),\\
F_{z3} &= mgL_f/2\left(L_f+L_r\right)+m\dot{u}h/2\left(L_f+L_r\right)\\
&\quad -\ m\dot{v}hL_f/b\left(L_f+L_r\right),\\
F_{z4} &= mgL_f/2\left(L_f+L_r\right)+m\dot{u}h/2\left(L_f+L_r\right)\\
&\quad +\ m\dot{v}hL_f/b\left(L_f+L_r\right),
\end{aligned}
\tag{27}
$$

where, g represents the gravitational acceleration; h denotes the distance from the vehicle's mass center to the ground.

The slip angles of each tire α_i ($i = (1–4)$ can be described as [28]:

$$\alpha_1 = -\delta_f + \arctan\left(\frac{v+\gamma l_f}{u-0.5b\gamma}\right), \tag{28}$$

$$\alpha_2 = -\delta_f + \arctan\left(\frac{v+\gamma l_f}{u+0.5b\gamma}\right), \tag{29}$$

$$\alpha_3 = -\arctan\left(\frac{v-\gamma l_r}{u-0.5b\gamma}\right), \tag{30}$$

$$\alpha_4 = -\arctan\left(\frac{v-\gamma l_r}{u+0.5b\gamma}\right). \tag{31}$$

For simultaneous longitudinal and lateral tire slip conditions, the combined tire forces and are formulated as [29]:

$$
\begin{aligned}
F_x &= F_{x0}\sigma_x/\sqrt{\sigma_x^2+\sigma_y^2},\\
F_y &= F_{y0}\sigma_y/\sqrt{\sigma_x^2+\sigma_y^2},\\
\sigma_x &= \left|s/(1+s)\right|, \quad \sigma_y = \left|\tan\alpha/(1+s)\right|.
\end{aligned}
\tag{32}
$$

According to the tire model, the tire force characteristics during vehicle operation are shown in Fig. 11.

4.3. Motor system model

In this paper, both the TV motor and the main drive motor are permanent magnet synchronous motors (PMSM), which are controlled using the common space vector pulse width modulation (SVPWM) method [30], and the motor control process block diagram is shown in Fig. 12. The motor control system is a complex multi-physics field system composed of a motor body, inverter and control algorithm, which involves many fields such as mechanism, electromagnetics, etc.

At present, the motor control algorithm based on SVPWM is a relatively mature technology. This paper focuses on the working mechanism of TVDa, taking the motor as an ideal power output source and only considering its torque dynamic response performance. To reduce the complexity of establishing and calculating the TVDa motor system mathematical model, the complex motor control process shown in Fig. 12 can be represented in the form of a dynamic transfer function, as presented in Fig. 13.

As also shown in Fig. 13, the open-loop transfer function of the motor q-axis current control system can be expressed as:

$$G_{iq\_\text{open}}(s) = \frac{i_q}{i_{d\_q}} = \frac{K_p(\tau_c s+1)}{\tau_c s}\cdot\frac{1}{T_s s+1}\cdot\frac{1}{Lq_s+R_q}, \tag{33}$$

where, i_q and i_{d_q} represent the actual and required current of the q-axis, respectively; K_p is the coefficient of the current loop proportional controller; τ_c is the integral time constant; T_s is the SVPWM switching time period; L_q is the q-axis inductance; R_q is the stator resistance.

Usually, the zero point of the current controller is designed to cancel out the motor poles, that is $\tau_c = L_q/R_q$. Equation (33) can be simplified as:

$$G_{iq\_\text{open}}(s) = \frac{i_q}{i_{d\_q}} = \frac{K_p}{s(T_s s+1)}, \tag{34}$$

Therefore, the closed-loop transfer function of the motor control system can be expressed as:

$$
\begin{aligned}
G_{iqn}(s) &= \frac{i_q}{i_{d\_q}}\\
&= \frac{K_p/[s(T_s s+1)]}{1/(T_f s+1)+K_p/[s(T_s s+1)]},
\end{aligned}
\tag{35}
$$

where, T_f is the current sampling time.

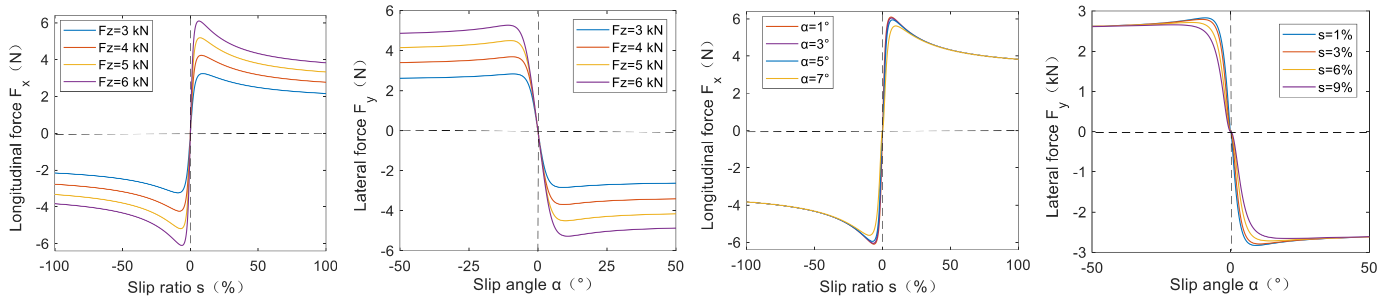

(a) Pure longitudinal force (b) Pure lateral force (c) Combined longitudinal force (d) Combined lateral force

Fig. 11. Magic Formula tire model

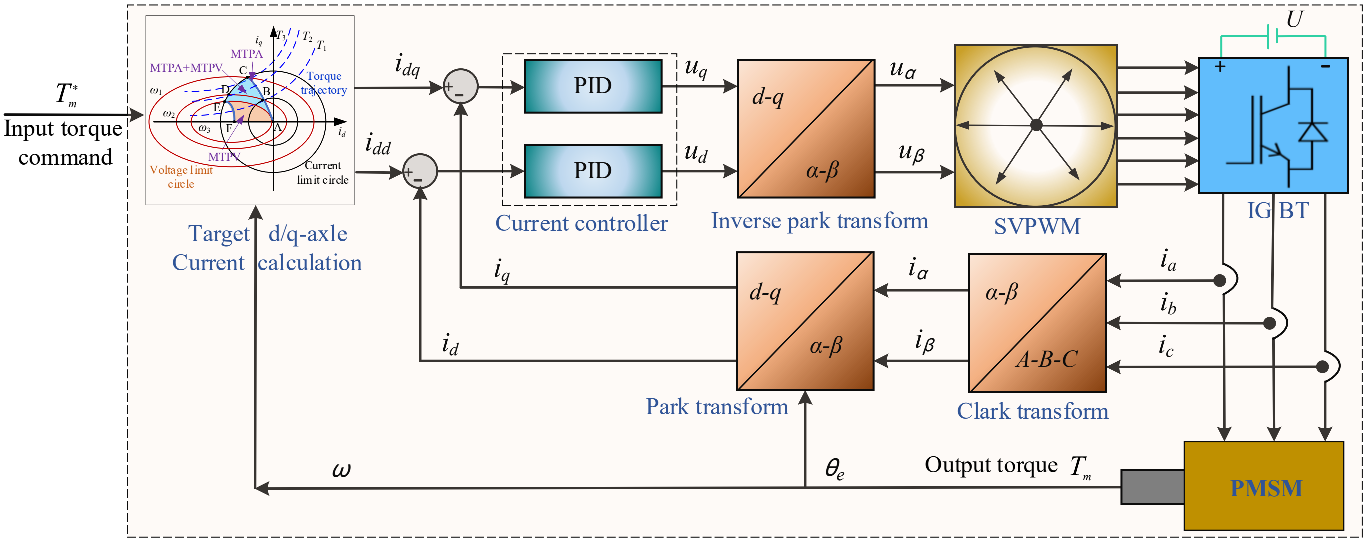

Fig. 12. Motor control process block diagram

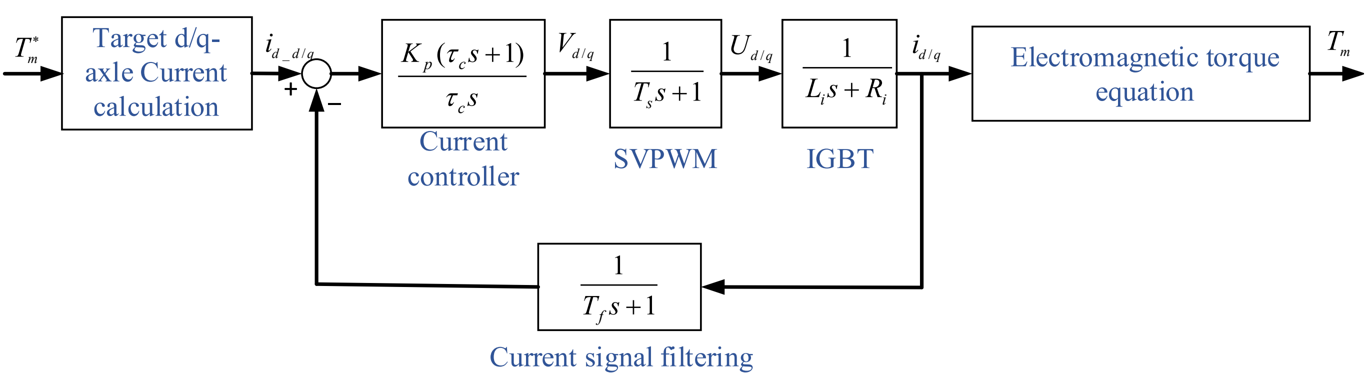

Fig. 13. Dynamic transfer function model of motor control system

When the current sampling time factor is ignored, that is $T_f \approx 0$, the motor closed-loop control system can be further approximately simplified as [31]:

$$\frac{T_m(s)}{T_m^*(s)} = \frac{i_q}{i_{dq}} = \frac{1}{2\xi^2 s^2 + 2\xi s + 1}, \tag{36}$$

where, ξ stands for the motor characteristic parameters; T_m is the motor output torque; T_m^* is the motor input torque command.

5. FUNCTIONAL VERIFICATION AND DISCUSSION OF TVDA

According to the vehicle dynamics formula derived in Section 4, a virtual prototype model is developed using SimulationX software. As illustrated in Fig. 14, the SimulationX interface incorporates a complete vehicle model featuring front wheel steering control, with the novel TVDa system implemented on the rear axle, and the vehicle parameter is described in Table 1.

5.1. Feasibility verification of improving vehicle steering maneuverability

One of the main functions of the novel TVDa is to promote the handling stability and steering maneuverability of the vehicle during cornering, which is effected through the transfer of the driving torque between inter-wheels. To verify the feasibility of TVDa in changing the steering performance of vehicles, the simulation condition is set as follows: the vehicle accelerates in a straight line within first to 10 seconds, and turns left after the 10th second, the curve of the steering wheel input angle converted into the front wheel angle through the transmission system is presented in Fig. 15a; the power source motor output torque curve during the whole simulation process is presented in Fig. 15b.

The yaw rate and turning radius of vehicles are the most important indicators for evaluating steering performance, and the open-loop simulation result of the vehicle's steering characteristics is presented in Fig. 16.

As illustrated in Fig. 16a, when the output torque of TV motor is −15 Nm, the inside wheel driving torque (left-half shaft) is

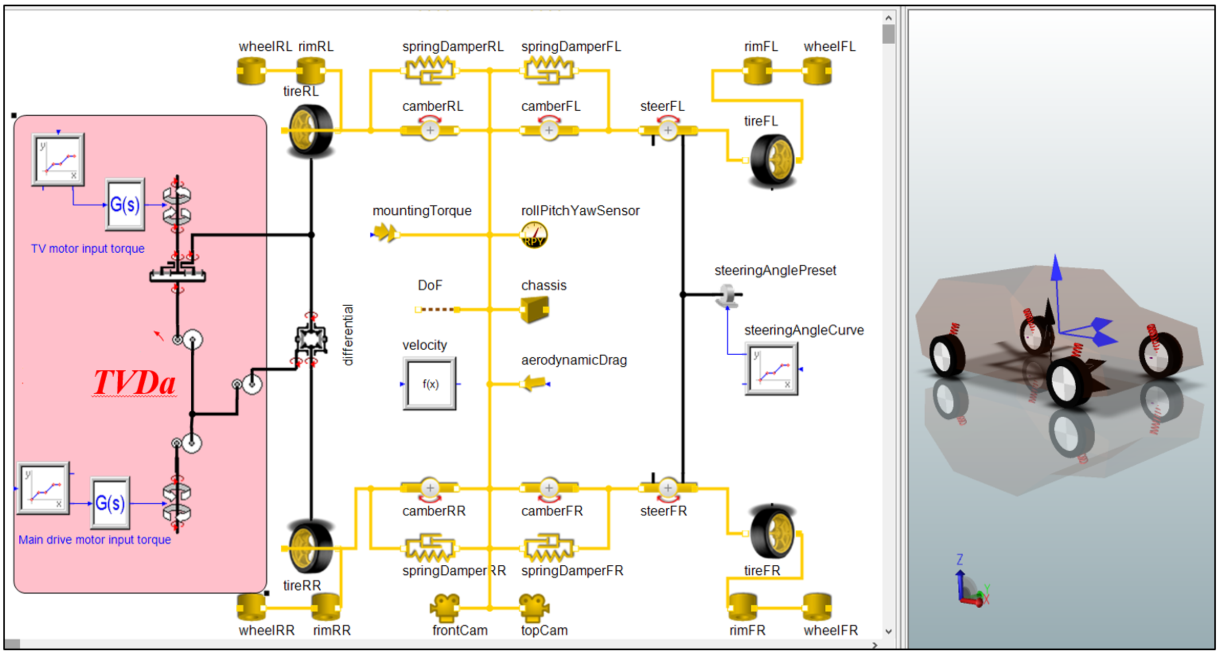

Fig. 14. Vehicle virtual prototype mode

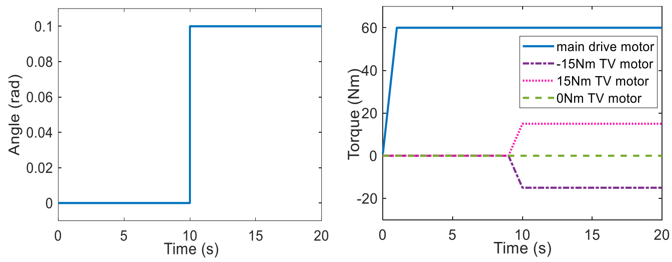

(a) front wheel input angle

(b) motor input torque

Fig. 15. Input curve of simulation condition

transferred to the outside wheel (right-half shaft), and an additional yaw moment is generated at this time, which is conducive to the vehicle's steering motion. Therefore, under the steering wheel input the angle remains unchanged and the vehicle's turning radius is smaller, which means the vehicle's steering flexibility is better. As illustrated in Fig. 16b, the TV motor output torque can change the vehicle's yaw rate. When the output torque of TV motor is -15 Nm, the steering yaw movement of vehicles is effectively improved, and the yaw rate increases. In contrast, when the TV motor output torque is 15 Nm, the driving torque of the outside wheel is transferred to the inside wheel. At that time, a yaw moment is generated that is not conducive to the yaw motion of vehicle, which increases the vehicle's turning radius and decreases the yaw rate, leading to an understeering trend in the vehicle and increasing the handling stability margin.

In summary, the research results indicate that the novel TVDa can significantly affect steering maneuverability and handling stability, which generates additional yaw moment required for the vehicle steering motion by controlling the output torque of the TV motor.

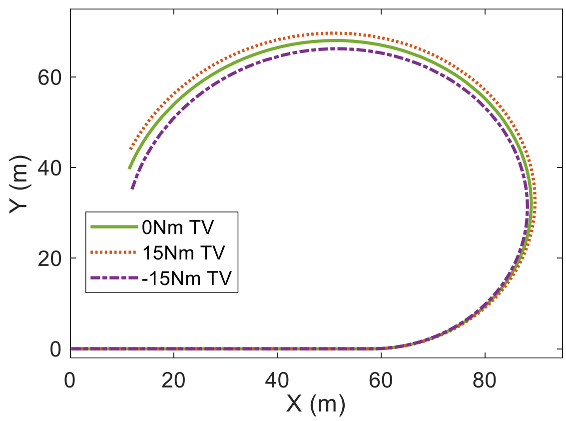

(a) drive trajectory

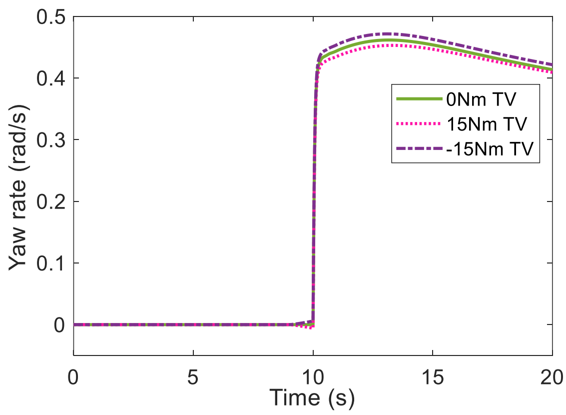

(b) yaw rate

Fig. 16. Effect of TVDa on vehicle's steering characteristics

5.2. Feasibility verification of improving vehicle trafficability

When the vehicle is driving on μ-split road or off-road pavement (the μ-split road is a special road condition where the road adhesion coefficients of the left and right wheels are significantly different), with the adhesion coefficient of the pavement on the two sides being inconsistent, the wheels on the low adhesion side would tend to slip while the wheels on the high adhesion side would run normally. When the TV motor operates in torque control mode, the TV motor output torque can be controlled to transfer wheel torque from the low adhesion coefficient road to the high adhesion side, so as to avoid the wheel slipping, and to improve the vehicle's power performance. According to the above theoretical analysis of (10) and the simulation result of Fig. 6, when the TV motor operates in speed control mode, the TV motor speed is actively kept at zero, that is, the TV motor is actively locked and the two-side half shafts rotational speed can be kept consistent. At this time, the TVDa can realize a function similar to the Audi TORSEN mechanical differential lock, which prevents wheel slipping on the low adhesion road and improves trafficability of vehicle.

To verify the effect of the TV motor two control modes on vehicle trafficability and power performance, the open-loop simulation conditions are set as follows: the vehicle starts to accelerate in a straight line from standstill on the μ-split road, that is, the road adhesion coefficient of left-side wheels is 0.2, while the right wheels is 1.0; the steering wheel angle remains zero, the main drive motor output torque can be seen in Fig. 17a; when the TV motor is working in the speed control mode, the motor speed remains zero; when the TV motor is working in the torque control mode, the output torque curve can be found in Fig. 17b.

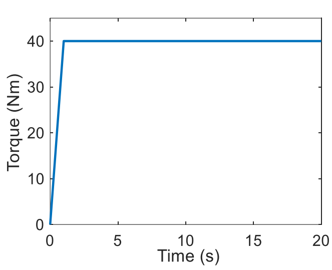

(a) main drive motor

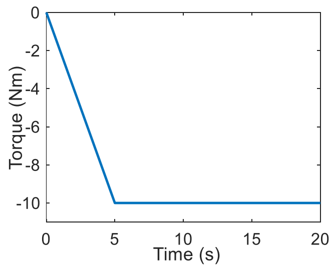

(b) TV motor

Fig. 17. Torque input curve of the motor

The open-loop simulation results are illustrated in Fig. 17. In Fig. 18a, when there is no control, the left wheel appears to be slipping, while the slip ratio of the right wheel is small and without slipping. After the TV motor is controlled by the torque mode and speed mode, respectively, the left wheel slipping trend is quickly restrained, and the drive anti-slip response is faster under the TV motor speed control mode. As shown in Fig. 18b, the maximum speed after simulation is 53 km/h when the TV motor remains without control. In the speed control mode and torque control mode, the maximum speed reaches about 56.8 km/h and the power performance of the vehicle increases by 7.2%. The simulation results indicate that the novel TVDa can effectively avoid the wheel slipping by actively controlling the speed or torque of the TV motor, and promoting the vehicle's power performance and trafficability on bad roads.

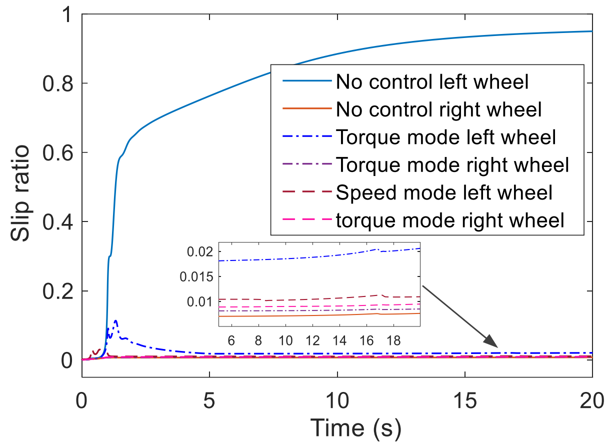

(a) wheel slip ratio

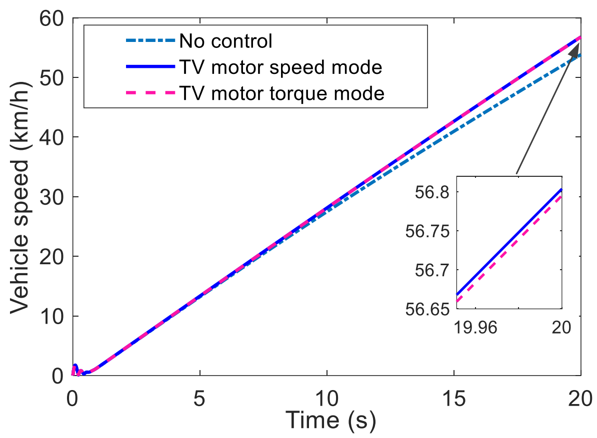

(b) vehicle speed

Fig. 18. Simulation result of the influence of TVDa on vehicle trafficability

It should be specifically noted that while actively locking the TV motor can rapidly suppress wheel slip, this mode induces significant heat generation in the motor. Consequently, TV motor locking is only suitable for short-duration anti-slip control. In contrast, torque transfer and distribution between bilateral wheels can be achieved by regulating the TV motor output torque, which has greater practical value for prolonged vehicle slip control applications.

5.3. Comparison between the novel TVDa and ESC

(1) Vehicle dynamics performance comparison

To compare the application effects of the novel TVDa with the traditional ESC, the verification test condition is set as follows: the main drive motor torque remains constant to enable the vehicle to accelerate (as shown in Fig. 15(b)); and the front wheel angle is illustrated in Fig. 15a; a differential torque of

100 Nm is applied to the bilateral wheels, generated by the driving torque distribution of TVDa and the braking torque distribution of ESC, respectively.

As presented in Fig. 19a, ESC generates a torque differential between the bilateral wheels by braking force distribution control, which inevitably reduces the total driving torque. In contrast, the TVDa system generates the required torque difference while maintaining constant total driving torque. Figure 19b demonstrates that the vehicle speed with TV control closely matches the uncontrolled case. However, when ESC is applied, the maximum achievable speed under simulation conditions is limited to 60 km/h. Notably, this ESC implementation results in a 9.1% reduction in power performance as compared to TVDa system. As illustrated in Fig. 19c and 19d, both TVDa and ESC can reduce the turning radius of vehicles and increase the yaw rate. Compared with the TVDa, the vehicle's turning radius after ESC control is smaller and the yaw rate is larger. The main reason for this is that the vehicle speed controlled by ESC is lower.

In summary, although ESC can allow the vehicle to have better turning ability, it would reduce the vehicle speed and affect the power performance of the vehicle. TVDa can effectively improve turning maneuverability of the vehicle without affecting the power performance, which results in better driving experience.

(2) Energy consumption analysis

According to the above analysis, torque application by the TV motor would induce additional energy dissipation, adversely affecting the vehicle's energy efficiency. And the ESC system also consumes energy in the process of applying braking force to wheels. Under the simulation conditions presented in Fig. 18, the comparison of energy consumption characteristics between ESC and TVDa is shown in Fig. 20.

As presented in Fig. 20, due to the small speed difference between the two-side wheels during cornering, the power of the TV motor is small, and the energy consumption is only 0.15J. Energy consumption of the ESC system in the whole working process is 14.5 J, which is about 12.8% of the energy consumption of the main drive motor. In summary, the TV motor achieves notable vehicle steering performance improvement with minimal energy consumption, exhibiting higher energy efficiency than ESC in stability control. This energy-efficient characteristic suggests promising potential for engineering applications.

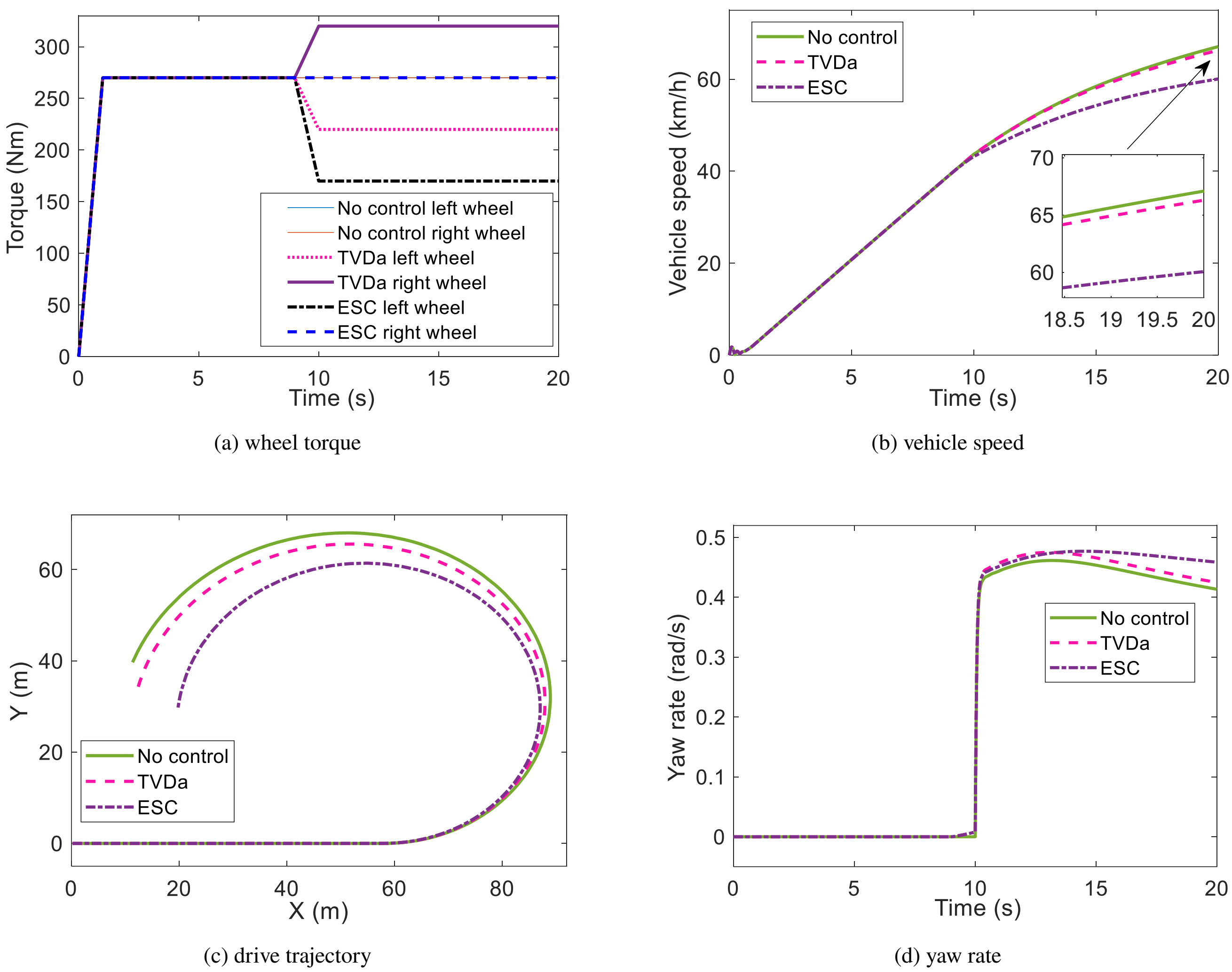

(a) wheel torque

(b) vehicle speed

(c) drive trajectory

(d) yaw rate

Fig. 19. Comparison of simulation results between TVDa and ESC

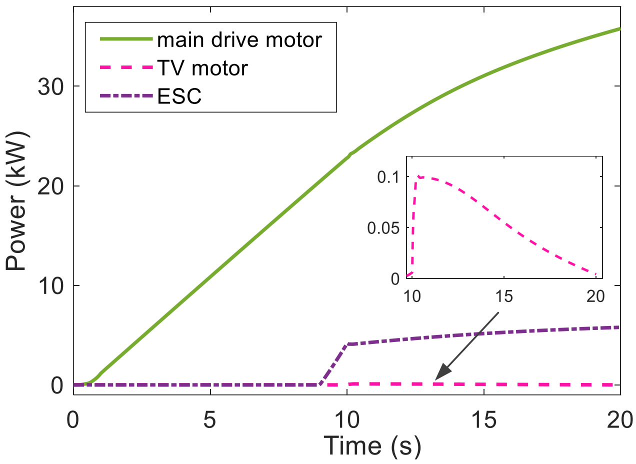

(a) power

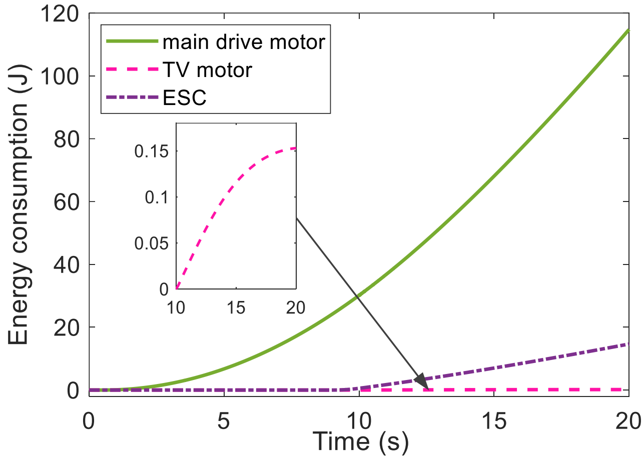

(b) energy consumption

Fig. 20. Comparison of energy consumption characteristics between ESC and TVDa

5.4. Discussion on the application of TVDa in traditional internal combustion engine vehicles

Nowadays, the global sale of electric vehicles have exceeded 20 million units, accounting for approximately 25% of total global car sales. However, the automobiles powered by internal combustion piston engines still constitute the majority of vehicles on the roads at present. Therefore, how to apply the novel TVDa structure configuration proposed in this paper on the basis of traditional internal combustion engine vehicles is an issue worthy of consideration.

Through the analysis of the structural design principles and working mechanism of the proposed TVDa in Section 2, it can be concluded that TVDa utilizes an additional TV motor to transfer and distribute the driving torque output by the main power source between the two-side wheels without changing the total driving force. Therefore, if the main drive motor of TVDa is replaced with an internal combustion engine, the proposed technical scheme can theoretically be applied to traditional fuel vehicles. Figure 21 shows two typical application cases of the proposed TVDa in traditional internal combustion engine vehicles.

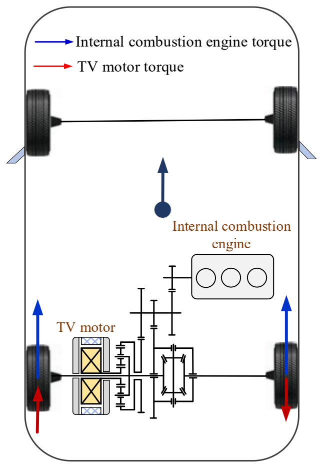

(a) integrated layout

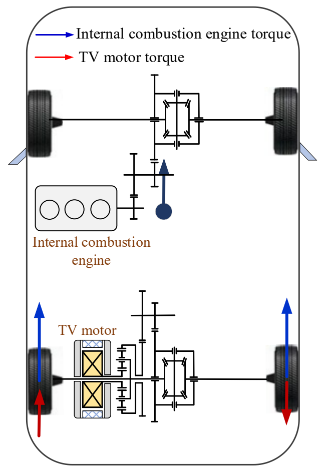

(b) distributed layout

Fig. 21. Application cases of TVDa in traditional internal combustion engine vehicles

However, it is worth noting that due to the proposed structure, configuration cannot avoid the application of motors, and additional batteries need to be added as energy sources when applying traditional fuel vehicles, which may lead to an increase in the manufacturing cost of the vehicle. Therefore, the author believes that the proposed TVDa is more suitable for application in traditional hybrid fuel vehicles.

6. CONCLUSIONS

The research and analysis of this study has allowed us to draw the following conclusions:

1. This paper proposes a novel TVDa configuration scheme for electric vehicles. Theoretical analysis and virtual prototype simulations confirm that the proposed TVDa enables arbitrary torque transfer and distribution between the left and right wheels while maintaining constant total driving torque. Moreover, by avoiding the use of clutches, TVDa offers advantages such as higher transmission efficiency and greater reliability as compared to traditional TVDs.
2. SimulationX-based virtual prototype simulations confirm that the proposed TVDa enhances vehicle handling stability and off-road performance via precise TV motor control, with negligible additional energy consumption. Compared with the traditional ESC, TVDa exhibits superior vehicle steering maneuverability retention capability and lower energy consumption, indicating strong potential for engineering applications.

In the future, we are going to manufacture the experimental prototype of TVDa and carry out the bench and real vehicle tests to verify the engineering practical value of TVDa.

ACKNOWLEDGEMENTS

This work was supported by the National Natural Science Foundation of China (Grant No. 52505268), the Shandong Provincial Natural Science Foundation (Grant No. ZR2024QE509, ZR2024QB152 and ZR2024ME089), Shandong Province Technology Small and Medium-Sized Enterprises Innovation Capability Enhancement Project (Grant No. 2024TSGC0279) and China Postdoctoral Science Foundation (Grant No. 2024 M761574).

REFERENCES

[1] C.S. Kim, K.S. Hong, and M.K. Kim, "Nonlinear robust control of a hydraulic elevator: Experiment-based modeling and two-stage Lyapunov redesign," *Control Eng. Pract.*, vol. 13, no. 5, pp. 789–803, 2005, doi: 10.1016/j.conengprac.2004.09.003.

[2] Xu. D, Xu. JC, Cui. XM, Zhou. Y, Sun. XY, and Wang. ZQ, "Handling stability analysis of decoupling suspension for formula racing," *Bull. Pol. Acad. Sci. Tech. Sci.*, vol. 73, p. e153829, 2025, doi: 10.24425/bpasts.2025.153829.

[3] JN. Wang, SL. Gao, K. Wang, Y. Wang, and QS. Wang, "Wheel torque distribution optimization of four-wheel independent-drive electric vehicle for energy efficient driving," *Control Eng. Pract.*, vol. 110, p. 104779, 2021, doi: 10.1016/j.conengprac.2021.104779.

[4] J. Kim, D.G. Nguyen, S. Park, M. Woo, D. Kim, and K.Y.S. Han, "Data-driven Vehicle Torque Vectoring Control Using Streaming Gaussian Process MPC," *Int. J. Control Autom. Syst.*, vol. 70, no. 12, pp. 3501–3512, 2025, doi: 10.1007/s12555-025-0483-x.

[5] S. Park, J. Kim, D.G. Nguyen, M. Woo, D. Kim, and K. Han, "Hierarchical NMPC for energy-efficient torque vectoring in four in-wheel motor electric vehicles," *Control Eng. Pract.*, vol. 164, p. 106477, 2025, doi: 10.1016/j.conengprac.2025.106477.

[6] J. Wang, Q. Wang, L. Jin, and C. Song, "Independent Wheel Torque Control of 4WD Electric Vehicle for Differential Drive Assisted Steering," *Mechatronics*, vol. 21, pp. 63–76, 2011, doi: 10.1016/j.mechatronics.2010.08.005.

[7] S. Gao, J. Wang, C. Guan, Z. Zhou, and Z. Liu, "Dynamic Characteristic Modeling and RBF-SMC Based Torque Control of a Novel Torque Vectoring Drive-Axle for Electric Vehicles," *IEEE Trans. Veh. Technol.*, vol. 74, no. 4, pp. 5757–5770, 2025, doi: 10.1109/TVT.2024.3507923.

[8] L. Sawaqed and I.H. Rabbaa, "Fuzzy Yaw Rate and Sideslip Angle Direct Yaw Moment Control for Student Electric Racing Vehicle with Independent Motors," *World Electr. Veh. J.*, vol. 13, p. 109, 2022, doi: 10.3390/wevj13070109.

[9] SL. Gao, JN. Wang, CY. Guan, ZD. Zhou, and Z. Liu, "Wheel Torque Distribution Control Strategy for Electric Vehicles Dynamic Performance With an Electric Torque Vectoring Drive Axle," *IEEE Trans. Transp. Electrif.*, vol. 10, no. 1, pp. 1692–1705, 2024, doi: 10.1109/TTE.2023.3267817.

[10] A. Usman and A. Saxena, "Technical Roadmaps of Electric Motor Technology for Next Generation Electric Vehicles," *Machines*, vol. 13, p. 156, 2025, doi: 10.3390/machines13020156.

[11] K. Tomo and S. Kaoru, "Classification and Analysis of Electric-Powered Lateral Torque-vectoring Differentials," *Proc. Inst. Mech. Eng., Part D: J. Automob. Eng.*, vol. 226, no. 6, pp. 713–724, 2012, doi: 10.1177/0954407011430182.

[12] Z.J. Zhang, Y.M. Cai, and D.F. Zhang, "Solving Ordinary Differential Equations with Adaptive Differential Evolution," *IEEE Access*, vol. 8 pp. 128908–128922, 2020, doi: 10.1109/ACCESS.2020.3008823.

[13] T.X. Pang, P.S. Yan, and H.H. Zhou, "Asymptotically Efficient Parameter Estimation for Ordinary Differential Equations," *Sci. Chin. Math.*, vol. 60, pp. 2263–286, 2017, doi: 10.1007/s11425-017-9155-0.

[14] A. Suhane, R.S. Rana, and R. Purohit, "Prospects of Torsen Differential in Four Wheel Drive Automobile Transmission System," *Mater. Today-Proc.*, vol. 15, no. 2, pp. 4036–4045, 2018, doi: 10.1016/j.matpr.2017.11.664.

[15] R. Russo, S. Strano, and M. Terzo, "Enhancement of Vehicle Dynamics Via an Innovative Magnetorheological Fluid Limited Slip Differential," *Mech. Syst. Signal Process.*, vol. 70, no. 71, pp. 1193–1208, 2016, doi: 10.1016/j.ymssp.2015.09.029.

[16] K. Sawase, and Inoue. K, "Classification and analysis of lateral torque-vectoring differentials using velocity diagrams," *Proc. Inst. Mech. Eng., Part D: J. Automob. Eng.*, vol. 222, no. 9, pp. 1527–1541, 2008, doi: 10.1243/09544070JAUTO824.

[17] N. Abidin, S. Imamori, and A. Alexander, "Development of High Efficiency next-generation SH-AWD Rear Drive Unit," *SAE Tech. Pap.*, vol. 01, p. 1098, 2015, doi: 10.4271/2015-01-1098.

[18] M. Dick, U. Hackenberg, and D. Isgen, "The audi R8: Motor sport technology for the road," *ATZextra Worldwide*, vol. 109, no. 2, pp. 2–7, 2007, doi: 10.1007/BF03224906.

[19] S. Frediani, R. Gianoglio, F. Giuliano, "System for the Active Control of a Motor Vehicle Differential," US Patent 6,393,351, May. 5, 2002.

[20] Yu. Chen, I. Chen, J. Chang, and L. Tyng, "Design and Analysis of a New Torque Vectoring System with a Ravigneaux Gearset for Vehicle Applications," *Energies*, vol. 10, p. 2157, 2017, doi: 10.3390/en10122157.

[21] C.K. Lin, P.J. Cheng, Y.J. Chung, and L. Tyng, "Conceptual Design and Analysis of Hybrid Torque-Vectoring Differential (H-TD)," *SAE Tech. Pap.*, vol. 01, p. 0333, 2019, doi: 10.4271/2019-01-0333.

[22] M. Diachuk and S.M. Easa, "Improved Mathematical Approach for Modeling Sport Differential Mechanism," *Vehicles*, vol. 4, no. 1, pp. 74–99, 2022, doi: 10.3390/vehicles4010005.

[23] A. Tahouni, M. Mirzaei, and B. Najjari, "Novel Constrained Nonlinear Control of Vehicle Dynamics Using Integrated Active Torque Vectoring and Electronic Stability Control," *IEEE Trans. Veh. Technol.*, vol. 68, no. 10, pp. 9564–9572, 2019, doi: 10.1109/TVT.2019.2933229.

[24] P. Dong, S.H. Wu, W. Guo, Y. Xu, S.H. Wang, and Y.H. Liu, "Coordinated Clutch Slip Control for the Engine Start of Vehicles with P2-hybrid Automatic Transmissions," *Mech. Mach. Theory*, vol. 153, p. 103899, 2020, doi: 10.1016/j.mechmach theory.2020.103899.

[25] D. Zinsmeister, T. Licklederer, F. Christange, P. Tzscheutschler, and V.S. Perić, "A Comparison of Prosumer System Configurations in District Heating Networks," *Energy Rep.*, vol. 7, pp. 430–439, 2021, doi: 10.1016/j.egyr.2021.08.085.

[26] J.N. Wang, S.L. Gao, Y. Qiang, M. Xu, C.Y. Guan, and Z.D. Zhou, "Structural Topology and Dynamic Response Analysis of an Electric Torque Vectoring Drive-Axle for Electric Vehicles," *Automot. Innov.*, vol. 5, no. 2, pp. 164–179, 2022, doi: 10.1007/s42154-022-00178-0.

[27] H.Y. Zhang and S. Yang, "Research on Race Car Steering Geometry Considering Tire Side Slip Angle," *Proc. Inst. Mech. Eng., Part P: J. Sports Eng. Technol.*, vol. 234, no. 1, pp. 72–87, 2020, doi: 10.1177/1754337119872417.

[28] W. Sun, J. Wang, Q. Wang, Assadian. F, and Fu. B, "Simulation Investigation of Tractive Energy Conservation for a Cornering Rear-wheel-independent-drive Electric Vehicle Through Torque Vectoring," *Sci. China Technol. Sci.*, vol. 61, pp. 257–272, 2018, doi: 10.1007/s11431-017-9139-5.

[29] D.J. Yin, J.J. Wang, J.J. Du, G. Chen, and J.S. Hu, "A New Torque Distribution Control for Four-Wheel Independent-Drive Electric Vehicles," *Actuators*, vol. 10, p. 122, 2021, doi: 10.3390/act10060122.

[30] X.Z. Xian, and Z.P. Yu, "SVPWM Modulation Algorithms in Motor Controller of Electric Vehicles," *J. Tongji Univ. (Nat. Sci.)*, vol. 45, no. 1, pp. 92–97, 2017, doi: 10.11908/j.issn.0253-374x.2017.01.014.

[31] J.N. Wang, Z. Liu, C.Y. Guan, Z.D. Zhou, B. Yang, and T.H. Zheng, "H_∞ Robust Control of a Novel Dual-Motor Drive System and Its Application on Stability Enhancement of Electric Vehicles via Torque Vectoring," *IEEE Trans. Transp. Electrific.*, vol. 11, no. 4, pp. 8889–8902, 2025, doi: 10.1109/TTE.2025.3565757.